Supplemental Material for *Plasmon dispersion in Graphite: A comparison of current* ab initio *methods*

Sean M. Anderson,[1] Bernardo S. Mendoza,[1] Giorgia Fugallo,[2] and Francesco Sottile[3,4]

[1] *Centro de Investigaciones en Óptica, León, Guanajuato, México*
[2] *CNRS, UMR 6607, Laboratorie de Thermique et Energie de Nantes (LTeN) Polytech'Nantes, Université de Nantes, Rue Christian Pauc, F-44306 Nantes Cedex 3, France*
[3] *Laboratoire des Solides Irradiés, École Polytechnique, CNRS, CEA, Université Paris-Saclay, F-91128 Palaiseau, France*
[4] *European Theoretical Spectroscopy Facility (ETSF)*

(Dated: May 9, 2019)

I. THE $\pi + \sigma$ PLASMON

Our theoretical calculations do not have to be limited to only the low energy range used in the experiments. The $\pi + \sigma$ plasmon that occurs in the 20 to 40 eV range retains its plasmonic character for momentum values up to $q \approx 1.5$ Å^{-1}. Figs. 1a and 1b depict the q-dependent dispersion in the 15 to 45 eV energy range for each calculated method, along the $\Gamma \rightarrow \mathrm{M}_4$ and $\Gamma \rightarrow \mathrm{K}_4$ paths, respectively. One crucial remark about these results concerns the number of bands included in each calculation; with the exception of the BSE CP calculation, all methods include 80 total bands in order to obtain well-converged results over the full energy range. The BSE CP calculation, due to the considerable computational expense of diagonalizing the complete Hamiltonian, only includes 20 total bands which is enough to obtain convergence for the low energy range of the π plasmon, but not enough for the high energy range presented here. Therefore, this data cannot be used for quantitative analysis, although the general trend can be readily visualized.

Available experimental data[1–3] shows that the $\pi + \sigma$ plasmon peak, for $q = 0$ Å^{-1}, is between 25 to 30 eV. As the value of q increases, the peak widens, decreases slightly in intensity, and moves towards higher energies. We find that this behavior is well reproduced with methods that include the coupling terms in the excitonic Hamiltonian, and our calculations predict that this plasmon continues to increase in width and decrease in intensity until almost fully dissipating at large values of q. The BSE CP calculation, as mentioned above, does not have enough bands included in order to reproduce the fine features and intensity of the peak. However, the general trend is the same. On the other hand, methods that use the Tamm-Dancoff approximation and neglect these coupling terms tell a different story altogether. These methods tend to substantially overestimate the peak energy position for low values of q, have an intensity that is several times larger than the experimental value, that very rapidly diminishes in intensity towards medium values of q. This behavior does not fit the aforementioned experimental data at all. The dispersive behavior of the $\pi + \sigma$ plasmon is very similar for both the $\Gamma \rightarrow \mathrm{M}_4$ and $\Gamma \rightarrow \mathrm{K}_4$ paths.

These plots mark a striking visual difference between using the full excitonic Hamiltonian and the TDA; the latter is simply not well-suited for describing the $\pi + \sigma$ plasmon. Overall, methods that include the coupling terms offer the best agreement with experiment; The BSE can accurately describe both exciton and plasmon excitations when used with the full Hamiltonian as the coupling terms are crucial for accurately describing the plasmon behavior.

II. BENCHMARKS

During the course of this study, we were able to gather a significant amount of real-world performance data for the purpose of benchmarking the different calculations. Table I presents the most general time metrics for each of the different methods featured in this work; these values include the entire calculation time, from reading the input files to writing the final datasets. The standard deviation (σ) for each value was determined from the multiple calculations required for each grid of **k**-points. In general, σ merely represents the normal fluctuations in clock speed and available resources that occur in any computing system. The compute nodes used in these benchamarks consist of three Intel Xeon E7-8860v3 platforms with clock speeds of 2.20 GHz. Each node has four processors for a total of 64 cores and 3 TB of DDR4 RAM memory.

These benchmarks make it clear that solving the BSE the full excitonic Hamiltonian implies an enormous leap in computational time; for this particular grid, the time is up to 5 orders of magnitude larger. Fortunately, this time can be greatly reduced by further parallelizing the number of **k**-points over more cores. As mentioned above, each of our compute nodes has 64 cores allowing us to parallelize over 192 cores total. Table II presents the duration (in days) of the full excitonic calculation for the 14×14×02 grid as a function of the number of cores. The total time is

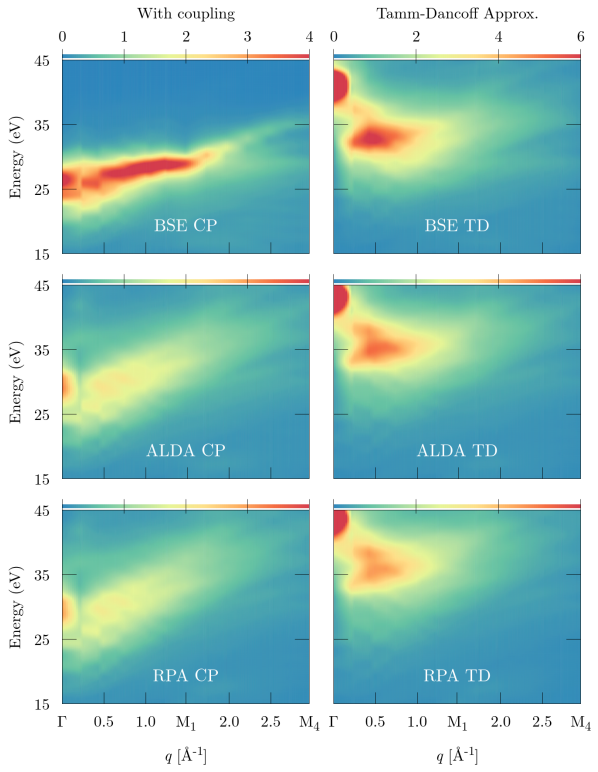

(a) q values along the $\Gamma \rightarrow \mathrm{M}_4$ path.

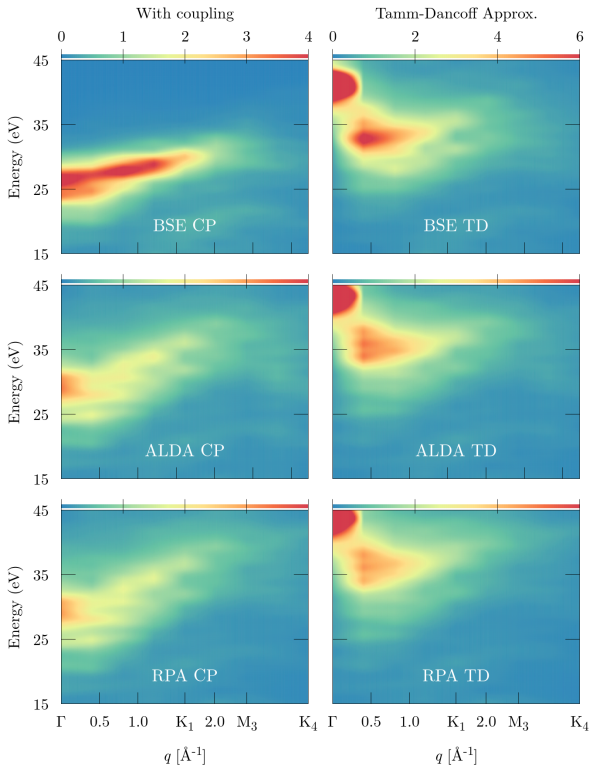

(b) q values along the $\Gamma \rightarrow \mathrm{K}_4$ path.

FIG. 1. Color map representations of the calculated EEL spectra vs. transfered momentum (q) for the $\pi + \sigma$ plasmon region. Methods including the coupling terms in the excitonic Hamiltonian are shown in the left column, and methods neglecting these terms (Tamm-Dancoff approximation) are shown in the right column. The EEL intensity is represented by the color palette ranging from blue to red.

reduced by around 50% by doubling the number of cores from 64 to 128 (at which point we more or less reach the scalability range of our code). This study is obviously not exhaustive as the number of cores used was not optimal; the 14×14×02 has 392 **k**-points which is not evenly divisible by 64, 128, or 192. However, we can clearly see that the parallelization is still very effective across two nodes, probably reaching peak efficiency at 98 cores with 4 **k**-points per core. However, as these numbers were obtained over the course of many trials and for such long calculations, emphasis was given on the number of simultaneous calculations possible rather than the most optimized parallelization for each one.

Lastly, the full excitonic calculation also has significant memory requirements that must be taken into consideration. The memory required for storing the excitonic Hamiltonian (in GB) can be calculated using the following expression,

$$(k_x \times k_y \times k_z \times N_v \times N_c)^2 \times \frac{8\,\text{bytes}}{1024^3}, \tag{1}$$

where k_x, k_y, and k_z define the **k**-point grid, and N_v and N_c are the number of valence and conduction bands, respectively. Fig. 2 depicts the relation from Eq. (1) (solid red line) using the left-side axis. The size of the excitonic Hamiltonian was around 300 GB for this work, with 80 total bands included for most calculations. The blue dots and dotted line are the raw calculation times (in hours) and the quartic fit for the BSE TD method. The reduced Hamiltonian in the TDA, coupled with the very efficient Haydock iterative scheme vastly reduces the calculation time compared to the BSE with the full Hamiltonian. However, calculation time still increases very rapidly with the number of bands; which is particularly troublesome for systems with spectral features present at high energies. Unfortunately, we are not able to provide this same benchmark for the BSE CP method, as calculation time became unwieldy above 20 total bands.

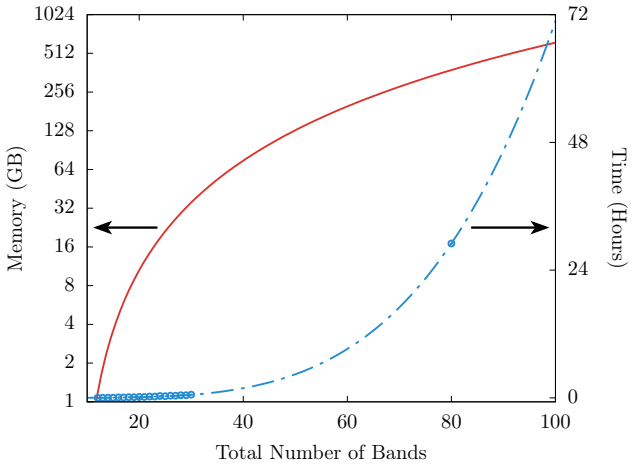

FIG. 2. Memory usage (in GB) as a function of the total number of bands (red solid line, left-hand scale), and calculation time as a function of the total number bands included in the BSE TD method for the 14x14x02 **k**-point grid, parallelized over 64 cores (blue circles, right-hand scale). The blue dotted line is a quartic fit, where $f(N) = 7.082 \times 10^{-7} N^4$ in hours.

TABLE I. Duration in minutes for each of the different levels of approximation for the 14×14×02 (392) grid of **k**-points, alongside the standard deviation and the number of cores used. A total of 20 bands were included in the calculation.

Method	Duration (min)	σ (min)	Cores
BSE CP	20559.13	472.52	64
BSE TD	40.05	0.32	64
ALDA CP	7.67	1.10	32
ALDA TD	1.90	0.17	32
RPA CP	3.35	0.43	32
RPA TD	1.63	0.25	32

TABLE II. Duration in days for each of the different levels of approximation for the 14×14×02 (392) grid of **k**-points, alongside the standard deviation and the number of cores used. A total of 20 bands were included in the calculation.

Cores	Duration (Days)	σ (Days)	**k**-points
64	14.3	0.33	392
128	7.4	0.00	392
192	7.8	0.21	392

[1] K. Zeppenfeld, Zeitschrift für Physik A Hadrons and nuclei **243**, 229 (1971).
[2] U. Büchner, Phys. Status Solidi B **81**, 227 (1977).
[3] A. G. Marinopoulos, L. Reining, A. Rubio, and V. Olevano, Phys. Rev. B **69**, 245419 (2004).